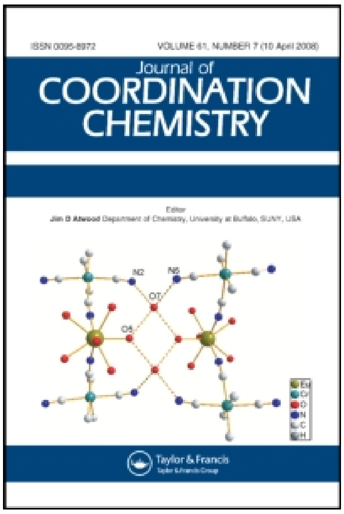

Journal of Coordination Chemistry
Publication details, including instructions for authors and subscription information:
http://www.informaworld.com/smpp/title~content=t713455674

Formation of 1-D ladder- and 2-D sheet-like networks due to stereospecific π-π stacking and hydrogen bonding between enantiomeric sulfur-bridged dinuclear complexes of penicillaminates

Yasunori Yamada[a]; Miyuki Kono[a]; Yusuke Miyoshi[a]; Toshihiro Nagasaki[a]; Masayuki Koikawa[a]; Tadashi Tokii[a]
[a] Faculty of Science and Engineering, Department of Chemistry and Applied Chemistry, Saga University, Saga 840-8502, Japan

First published on: 12 February 2010

Journal of Coordination Chemistry
Vol. 63, No. 5, 10 March 2010, 742–761

Formation of 1-D ladder- and 2-D sheet-like networks due to stereospecific π–π stacking and hydrogen bonding between enantiomeric sulfur-bridged dinuclear complexes of penicillaminates

YASUNORI YAMADA*, MIYUKI KONO, YUSUKE MIYOSHI, TOSHIHIRO NAGASAKI, MASAYUKI KOIKAWA and TADASHI TOKII

Faculty of Science and Engineering, Department of Chemistry and Applied Chemistry, Saga University, 1 Honjo-machi, Saga, Saga 840-8502, Japan

(*Received 20 August 2009; in final form 21 October 2009*)

Reaction of *trans*(N)-$[Co(\textsc{d}\text{-pen})_2]^-$ (pen = penicillaminate) or *trans*(N)-$[Co(\textsc{l}\text{-pen})_2]^-$ with $[MCl_2(L)]$ {M = Pd or Pt, L = 2,2′-bipyridine (bpy) or 1,10-phenanthroline (phen)} in the presence of tetrafluoroborate stereoselectively gave an optically active S-bridged dinuclear complex, $[M(L)\{Co(\textsc{d}\text{-pen})_2\}]BF_4 \cdot 2H_2O$ or $[M(L)\{Co(\textsc{l}\text{-pen})_2\}]BF_4 \cdot 2H_2O$. The mixture of equimolar amounts of these enantiomers in H_2O crystallizes as $[M(L)\{Co(\textsc{d}\text{-pen})_2\}]_{0.5}[M(L)\{Co(\textsc{l}\text{-pen})_2\}]_{0.5}BF_4 \cdot 4H_2O$ (DLbpyM $\cdot$ $4H_2O$, DLphenM-A $\cdot$ $4H_2O$), in which the enantiomeric complex cations are included by the ratio of 1 : 1. In crystals of DLbpyM $\cdot$ $4H_2O$ and DLphenM-A $\cdot$ $4H_2O$, $[M(L)\{Co(\textsc{d}\text{-pen})_2\}]^+$ and $[M(L)\{Co(\textsc{l}\text{-pen})_2\}]^+$ interact stereospecifically with each other through π-conjugated systems to form dimeric structures. Other racemic crystals with the same chemical compositions as DLphenM-A $\cdot$ $4H_2O$, DLphenM-B $\cdot$ $4H_2O$, were obtained from equimolar amounts of $[M(phen)\{Co(\textsc{d}\text{-pen})_2\}]^+$ and $[M(phen)\{Co(\textsc{l}\text{-pen})_2\}]^+$ in aqueous acetonitrile solution. In the crystals of DLphenM-B $\cdot$ $4H_2O$, $[M(phen)\{Co(\textsc{d}\text{-pen})_2\}]^+$ and $[M(phen)\{Co(\textsc{l}\text{-pen})_2\}]^+$ are arranged alternately while overlapping phen planes, and the π electronic systems of phen interact with each other. Although stereospecific hydrogen bonds between the coordinated $-NH_2$ and $-COO^-$ groups are formed in both DLphenM-A $\cdot$ $4H_2O$ and DLphenM-B $\cdot$ $4H_2O$, their bonding modes differ noticeably from each other. As a result, DLphenM-A $\cdot$ $4H_2O$ builds up 1-D ladder-like networks due to the stereospecific π–π stackings and hydrogen bondings between enantiomers, while 2-D sheet-like networks are established for DLphenM-B $\cdot$ $4H_2O$.

Keywords: Stereospecific interactions; Co(III)–Pd(II) and Co(III)–Pt(II) complexes; Phenanthroline complexes; Penicillaminate complexes; Crystal structures

1. Introduction

An octahedral metal chelated by plural β-aminoalkylthiolates acts as an S-donating bidentate metalloligand toward $[MX_2(bpy)]$ (M = Pd(II) or Pt(II), X = Cl^- or NO_3^-, bpy = 2,2′-bipyridine), in which the two X ligands are susceptible to substitutions by

*Corresponding author. Email: yyamada@cc.saga-u.ac.jp

Journal of Coordination Chemistry
ISSN 0095-8972 print/ISSN 1029-0389 online © 2010 Taylor & Francis
DOI: 10.1080/00958971003605767

other ligands, resulting in the formation of a dinuclear complex composed of a $[M(\mu{-}S)_2(bpy)]$ framework and an octahedral metal unit [1–7]. In the reaction of *fac*(*S*)-$[Co(aet)_3]$ (aet = 2-aminoethanethiolate) with $[PtCl_2(bpy)]$, for instance, a dinuclear complex, $[Pt(bpy)\{Co(aet)_3\}]^{2+}$, is formed [1]. A similar reaction of $[Ni\{Co(aet)_2(en)\}_2]^{4+}$ (en = ethylenediamine), in which two terminal *cis*(*S*)-$[Co(aet)_2(en)]^+$ units can be regarded as bidentate S-donors, with $[PtCl_2(bpy)]$ gives $[Pt(bpy)\{Co(aet)_2(en)\}]^{3+}$ [1]. Two absolute configurations, Δ and Λ, are possible for such octahedral S-donating metal units, and hence these dinuclear complexes are obtained as racemic crystals. In contrast to the above racemic $[Ni\{Co(aet)_2(en)\}_2]^{4+}$, an optically active trinuclear analog, $\Delta\Delta$-$[Ni\{Co(aet)_2(R\text{-pn})\}_2]^{4+}$ (pn = 1,2-propanediamine), reacts with $[MX_2(bpy)]$ to form Δ-$[M(bpy)\{Co(aet)_2(R\text{-pn})\}]^{3+}$ stereoselectively [2, 3]. A similar optically active S-bridged dinuclear complex, $[M(bpy)\{Co(D\text{-pen})_2\}]^+$ (pen = penicillaminate), is preferentially derived from the bidentate metalloligand, *trans*(*N*,*O*,*S*)-$[Co(\textsc{d}\text{-pen})_2]$ [3]. While these optically active complexes exist as monomers in the crystalline states, the racemic complexes afford dimeric or higher dimensional linear-chain structures due to π–π stacking of the bpy frameworks in the dinuclear units [1–7]. This implies enantioselective interactions between the π frameworks, which are rather distant from the chiral center of the octahedral metal unit, in these dinuclear complexes. In fact, a mixture of equimolar amounts of $[Pt(bpy)\{Co(\textsc{d}\text{-pen})_2\}]Cl$ and $[Pt(bpy)\{Co(\textsc{l}\text{-pen})_2\}]Cl$ in H_2O crystallizes as the racemic $[Pt(bpy)\{Co(\textsc{d}\text{-pen})_2\}]_{0.5}[Pt(bpy)\{Co(\textsc{l}\text{-pen})_2\}]_{0.5}Cl$ with a linear-chain π–π stacking structure, in which two enantiomeric complex cations are arranged alternately [4]. Such an assembly induced by enantioselective π–π interactions significantly respond to hydrogen bonding abilities and/or steric factors of coexistent counter anions [6]. In racemic crystals of $[Pt(bpy)\{Co(\textsc{d}\text{-pen})_2\}]_{0.5}[Pt(bpy)\{Co(\textsc{l}\text{-pen})_2\}]_{0.5}X$ ($X = NO_3^-$, ClO_4^-, or I^-), for instance, a pair of enantiomeric complex cations affords a dimeric π–π stacking structure. In the crystal with $X = Br^-$, a similar linear-chained π–π stacking structure to the case of $X = Cl^-$ is built up with π–π stacking contacts between the enantiomers [6]. For S-bridged polynuclear complexes with aromatic diimine ligands, expansions of π electronic systems also impinge on assembled dimensionalities [8, 9]. In the tetranuclear Pd(II) complex systems, for instance, the phen (phen = 1,10-phenanthroline) complex, $[\{Pd(phen)\}_2\{Pd(aet)_2\}_2]^{4+}$, affords a linear-chain π–π stacking structure while the corresponding bpy complex, $[\{Pd(bpy)\}_2\{Pd(aet)_2\}_2]^{4+}$, shows a dimeric one. Furthermore, the use of other π frameworks provides diversified assembled structures even in conditions with the same counter anions [10]. Such diversity in assembly was illustrated by an example of the trinuclear complex, $[\{Pd(terpy)\}_2\{Pd(aet)_2\}]^{4+}$ (terpy = 2,2′:6′,2″-terpyridine), which crystallizes in two distinct assembly manners under the presence of BF_4^- [10]. It is speculated from these facts that adoptions of another diimine ligand (L) with expanded π electronic systems and/or diversity-carrying counter anions (X^-) for the $[M(L)\{Co(\textsc{d}\text{-pen})_2\}]_{0.5}[M(L)\{Co(\textsc{l}\text{-pen})_2\}]_{0.5}X$ systems provide more detailed information on responsibilities of diimine ligands and/or counter anions for such stereospecific assembly of the complexes. In this investigation, we have examined assemblies between the enantiomers, $[M(L)\{Co(\textsc{d}\text{-pen})_2\}]^+$ and $[M(L)\{Co(\textsc{l}\text{-pen})_2\}]^+$ (L = bpy, phen), from stereo- and spectro-chemical aspects with the aid of BF_4^- as a diversity-carrying counter anion.

2. Experimental

2.1. *Materials*

2,2′-Bipyridine, 1,10-phenanthroline hemihydrate, $CoCl_2 \cdot 6H_2O$ and $PdCl_2$ were obtained from Wako Pure Chemical Ind. Co., Ltd. K_2PtCl_4, D-penicillamine, and L-penicillamine were purchased from Tanaka Rare Metal Ind., Ltd., Tokyo Chemical Co., Ltd. and Aldrich Chemical Co., Inc., respectively. K[Co(D-pen)$_2$]$\cdot$2.5H_2O, K[Co(L-pen)$_2$]$\cdot$2.5H_2O, [$PdCl_2$(bpy)], [$PdCl_2$(phen)], [$PtCl_2$(bpy)], and [$PtCl_2$(phen)] were prepared by modified methods from the literature [11–14]. The other chemicals were purchased from Wako Pure Chemical Ind. Co., Ltd., Tokyo Chemical Co., Ltd., or Aldrich Chemical Co., Inc. All of the chemicals were of reagent grade and used without purification.

2.2. *Preparation of [M(bpy){Co(D-pen)$_2$}]BF_4 (DbpyM) and [M(bpy){Co(L-pen)$_2$}]BF_4 (LbpyM)*

To a reddish brown solution containing K[Co(D-pen)$_2$]$\cdot$2.5H_2O or K[Co(L-pen)$_2$]$\cdot$2.5H_2O (0.22 g, 0.5 mmol) in 25 cm^3 H_2O was added [MCl_2(bpy)] (0.5 mmol). The mixture was stirred at 55 °C for 1 h followed by cooling to room temperature. To the cooled solution was added $AgBF_4$ (0.19 g, 1.0 mmol) in 25 cm^3 CH_3CN. After removing precipitated AgCl by filtration, the filtrate was evaporated to dryness. The residue was re-dissolved in a minimum of H_2O and the solution was kept standing for several days. The resulting microcrystalline powder was collected by filtration.

DbpyPd $\cdot$ 2H_2O: yield = 0.26 g (70% based on Co). Anal. Calcd for $C_{20}H_{30}BN_4O_6F_4S_2CoPd$ (%): C, 32.52; H, 4.09; N, 7.58. Found (%): C, 32.51; H, 4.10; N, 7.50. ^{1}H-NMR (300 MHz, 1 : 1 mixed solvent of D_2O and CD_3CN), $\delta = 1.52$ (s, 6H, pen), 1.78 (s, 6H, pen), 3.69 (s, 2H, pen), 7.90 (t, 2H, bpy), 8.37 (t, 2H, bpy), 8.46 (d, 2H, bpy), 8.94 (d, 2H, bpy). UV-Vis spectrum in H_2O [ν_{max}, $10^3\,cm^{-1}$ ($\log \varepsilon$ ($mol^{-1}\,dm^3\,cm^{-1}$))]: 15.92 (1.83), 18.9 (2.0)^{sh}, 22.1 (2.6)^{sh}, 28.6 (3.8)^{sh}, 31.0 (4.1)^{sh}, 32.36 (4.20), 34.97 (4.21), 42.19 (4.61), 48.1 (4.5)^{sh}. CD spectrum in H_2O [ν_{max}, $10^3\,cm^{-1}$ ($\Delta\varepsilon$)]: 15.82 (−2.55), 19.49 (+10.27), 22.4 (−8.4)^{sh}, 25.58 (−17.61), 28.25 (−21.19), 32.15 (+48.66), 35.1 (+34.9) ^{sh}, 39.6 (+27.1)^{sh}, 42.92 (+46.97). Diffuse reflectance spectrum [ν_{max}, $10^3\,cm^{-1}$]: 15.72, 19.0^{sh}, 22.4^{sh}, 28.5^{sh}, 30.58, 31.7^{sh}; sh = shoulder.

LbpyPd $\cdot$ 2H_2O: yield = 0.27 g (73% based on Co). Anal. Calcd for $C_{20}H_{30}BN_4O_6F_4S_2CoPd$ (%): C, 32.52; H, 4.09; N, 7.58. Found (%): C, 32.52; H, 4.11; N, 7.48. ^{1}H-NMR (300 MHz, 1 : 1 mixed solvent of D_2O and CD_3CN), $\delta = 1.52$ (s, 6H, pen), 1.79 (s, 6H, pen), 3.70 (s, 2H, pen), 7.90 (t, 2H, bpy), 8.37 (t, 2H, bpy), 8.47 (d, 2H, bpy), 8.94 (d, 2H, bpy). UV-Vis spectrum in H_2O [ν_{max}, $10^3\,cm^{-1}$ ($\log \varepsilon$ ($mol^{-1}\,dm^3\,cm^{-1}$))]: 15.92 (1.85), 18.9 (2.1)^{sh}, 22.4 (2.7)^{sh}, 28.7 (3.8)^{sh}, 31.0 (4.1)^{sh}, 32.36 (4.22), 34.97 (4.23), 42.19 (4.63), 48.1 (4.6)^{sh}. CD spectrum in H_2O [ν_{max}, $10^3\,cm^{-1}$ ($\Delta\varepsilon$)]: 15.87 (+2.71), 19.46 (−10.62), 22.3 (+7.9)^{sh}, 25.38 (+17.43), 28.25 (+20.55), 32.15 (−50.88), 35.1 (−37.9)^{sh}, 39.9 (−30.0)^{sh}, 42.92 (−46.98). Diffuse reflectance spectrum [ν_{max}, $10^3\,cm^{-1}$]: 15.72, 19.0^{sh}, 22.4^{sh}, 28.5^{sh}, 30.58, 31.7^{sh}.

DbpyPt · 2H$_2$O: yield = 0.30 g (72% based on Co). Anal. Calcd for $C_{20}H_{30}BN_4O_6F_4S_2CoPt$ (%): C, 29.03; H, 3.65; N, 6.77. Found (%): C, 29.01; H, 3.64; N, 6.72. ^{1}H-NMR (300 MHz, 1 : 1 mixed solvent of D_2O and CD_3CN), $\delta = 1.50$ (s, 6H, pen), 1.66 (s, 6H, pen), 3.83 (s, 2H, pen), 7.95 (t, 2H, bpy), 8.45 (t, 2H, bpy), 8.50 (d, 2H, bpy), 9.08 (d, 2H, bpy). UV-Vis spectrum in H_2O [ν_{max}, $10^3\,cm^{-1}$ ($\log\varepsilon$ ($mol^{-1}\,dm^3\,cm^{-1}$))]: 16.34 (2.01), 19.31 (2.04), 25.0 $(3.1)^{sh}$, 28.3 $(3.6)^{sh}$, 31.25 (4.24), 32.36 (4.23), 37.1 $(4.2)^{sh}$, 41.49 (4.40), 49.38 (4.61). CD spectrum in H_2O [ν_{max}, $10^3\,cm^{-1}$ ($\Delta\varepsilon$)]: 16.16 (−4.57), 19.42 (+7.16), 22.1 $(-0.4)^{sh}$, 25.45 (−5.05), 28.1 $(+13.0)^{sh}$, 29.8 $(+13.9)^{sh}$, 30.86 (+15.27), 37.74 (+23.15), 44.64 (+32.82). Diffuse reflectance spectrum [ν_{max}, $10^3\,cm^{-1}$]: 16.03, 18.87, 25.2^{sh}, 28.3^{sh}, 30.76, 31.9^{sh}.

LbpyPt · 2H$_2$O: yield = 0.29 g (70% based on Co). Anal. Calcd for $C_{20}H_{30}BN_4O_6F_4S_2CoPt$ (%): C, 29.03; H, 3.65; N, 6.77. Found (%): C, 29.04; H, 3.65; N, 6.69. ^{1}H-NMR (300 MHz, 1 : 1 mixed solvent of D_2O and CD_3CN), $\delta = 1.50$ (s, 6H, pen), 1.66 (s, 6H, pen), 3.84 (s, 2H, pen), 7.95 (t, 2H, bpy), 8.44 (t, 2H, bpy), 8.50 (d, 2H, bpy), 9.08 (d, 2H, bpy). UV-Vis spectrum in H_2O [ν_{max}, $10^3\,cm^{-1}$ ($\log\varepsilon$ ($mol^{-1}\,dm^3\,cm^{-1}$))]: 16.21 (2.04), 19.31 (2.05), 25.1 $(3.2)^{sh}$, 28.2 $(3.7)^{sh}$, 31.25 (4.26), 32.36 (4.25), 37.0 $(4.2)^{sh}$, 41.32 (4.42), 49.38 (4.59). CD spectrum in H_2O [ν_{max}, $10^3\,cm^{-1}$ ($\Delta\varepsilon$)]: 16.10 (+4.89), 19.42 (−7.79), 22.9 $(+0.2)^{sh}$, 25.45 (+5.57), 28.0 $(-12.5)^{sh}$, 29.8 $(-15.2)^{sh}$, 30.86 (−16.37), 37.59 (−25.05), 44.64 (−35.58). Diffuse reflectance spectrum [ν_{max}, $10^3\,cm^{-1}$]: 16.00, 18.90, 25.2^{sh}, 28.3^{sh}, 30.76, 31.9^{sh}.

2.3. *Preparation of [M(bpy){Co(D-pen)$_2$}]$_{0.5}$[M(bpy){Co(L-pen)$_2$}]$_{0.5}$BF$_4$ (DLbpyM)*

An equimolar mixture of DbpyM (0.25 mmol) and LbpyM (0.25 mmol) was dissolved in a minimum of H_2O. After the solution was kept standing at room temperature for several days, the resulting crystals were collected by filtration.

DLbpyPd · 4H$_2$O: yield = 0.31 g (80% based on Co). Anal. Calcd for $C_{20}H_{34}BN_4O_8F_4S_2CoPd$ (%): C, 31.00; H, 4.42; N, 7.23. Found (%): C, 31.02; H, 4.43; N, 7.18. ^{1}H-NMR (300 MHz, 1 : 1 mixed solvent of D_2O and CD_3CN), $\delta = 1.52$ (s, 6H, pen), 1.79 (s, 6H, pen), 3.71 (s, 2H, pen), 7.90 (t, 2H, bpy), 8.37 (t, 2H, bpy), 8.94 (d, 2H, bpy), 9.03 (d, 2H, bpy). UV-Vis spectrum in H_2O [ν_{max}, $10^3\,cm^{-1}$ ($\log\varepsilon$ ($mol^{-1}\,dm^3\,cm^{-1}$))]: 15.92 (1.83), 18.9 $(2.0)^{sh}$, 22.1 $(2.6)^{sh}$, 28.6 $(3.8)^{sh}$, 31.0 $(4.1)^{sh}$, 32.36 (4.20), 34.97 (4.21), 42.19 (4.61), 48.1 $(4.5)^{sh}$. Diffuse reflectance spectrum [ν_{max}, $10^3\,cm^{-1}$]: 15.74, 21.5^{sh}, 28.7^{sh}, 30.76, 31.9^{sh}.

DLbpyPt · 4H$_2$O: yield = 0.35 g (81% based on Co). Anal. Calcd for $C_{20}H_{34}BN_4O_8F_4S_2CoPt$ (%): C, 27.82; H, 3.97; N, 6.49. Found (%): C, 27.80; H, 4.00; N, 6.41. ^{1}H-NMR (300 MHz, 1 : 1 mixed solvent of D_2O and CD_3CN), $\delta = 1.50$ (s, 6H, pen), 1.66 (s, 6H, pen), 3.82 (s, 2H, pen), 7.95 (t, 2H, bpy), 8.44 (t, 2H, bpy), 8.50 (d, 2H, bpy), 9.08 (d, 2H, bpy). UV-Vis spectrum in H_2O [ν_{max}, $10^3\,cm^{-1}$ ($\log\varepsilon$ ($mol^{-1}\,dm^3\,cm^{-1}$))]: 16.23 (2.02), 19.42 (2.03), 25.1 $(3.2)^{sh}$, 28.4 $(3.7)^{sh}$, 31.25 (4.25), 32.36 (4.23), 37.2 $(4.2)^{sh}$, 41.32 (4.40), 49.38 (4.59). Diffuse reflectance spectrum [ν_{max}, $10^3\,cm^{-1}$]: 16.00, 19.08, 27.1^{sh}, 30.76, 31.9^{sh}.

2.4. *Preparation of [M(phen){Co(D-pen)$_2$}]BF$_4$ (DphenM) and [M(phen){Co(L-pen)$_2$}]BF$_4$ (LphenM)*

The same synthetic procedure was employed as for preparation of DbpyM or LbpyM, except that $[MCl_2(phen)]$ was used instead of $[MCl_2(bpy)]$, and the reaction was induced in a 1 : 1 mixed solvent of CH_3OH and H_2O.

DphenPd · 2H$_2$O: yield = 0.28 g (73% based on Co). Anal. Calcd for $C_{22}H_{30}BN_4O_6F_4S_2CoPd$ (%): C, 34.64; H, 3.96; N, 7.34. Found (%): C, 34.66; H, 4.00; N, 7.29. ^{1}H-NMR (300 MHz, 1 : 1 mixed solvent of D_2O and CD_3CN), $\delta = 1.59$ (s, 6H, pen), 1.82 (s, 6H, pen), 3.76 (s, 2H, pen), 8.21 (t, 2H, phen), 8.27 (s, 2H, phen), 8.95 (d, 2H, phen), 9.26 (d, 2H, phen). UV-Vis spectrum in H_2O [ν_{max}, $10^3\,cm^{-1}$ ($\log\varepsilon$ ($mol^{-1}\,dm^3\,cm^{-1}$))]: 15.85 (1.85), 19.2 (2.1)^{sh}, 22.8 (2.8)^{sh}, 28.41 (3.87), 29.76 (3.88), 31.3 (4.0)^{sh}, 33.6 (4.2)^{sh}, 35.59 (4.50), 42.7 (4.6)^{sh}, 45.25 (4.72), 49.01 (4.69). CD spectrum in H_2O [ν_{max}, $10^3\,cm^{-1}$ ($\Delta\varepsilon$)]: 15.80 (− 2.40), 19.42 (+9.81), 22.3 (−7.0)^{sh}, 25.5 (−16.4)^{sh}, 27.86 (−17.42), 31.9 (+32.5)^{sh}, 33.1 (+37.5)^{sh}, 35.84 (+88.39), 41.8 (+35.0)^{sh}, 44.05 (+48.93), 48.08 (+27.74). Diffuse reflectance spectrum [ν_{max}, $10^3\,cm^{-1}$]: 15.63, 19.1^{sh}, 22.4^{sh}, 28.09, 29.4^{sh}, 30.9^{sh}, 32.7^{sh}, 35.0^{sh}.

LphenPd · 2H$_2$O: yield = 0.26 g (68% based on Co). Anal. Calcd for $C_{22}H_{30}BN_4O_6F_4S_2CoPd$ (%): C, 34.64; H, 3.96; N, 7.34. Found (%): C, 34.63; H, 3.98; N, 7.31. ^{1}H-NMR (300 MHz, 1 : 1 mixed solvent of D_2O and CD_3CN), $\delta = 1.59$ (s, 6H, pen), 1.82 (s, 6H, pen), 3.75 (s, 2H, pen), 8.20 (t, 2H, phen), 8.27 (s, 2H, phen), 8.95 (d, 2H, phen), 9.25 (d, 2H, phen). UV-Vis spectrum in H_2O [ν_{max}, $10^3\,cm^{-1}$ ($\log\varepsilon$ ($mol^{-1}\,dm^3\,cm^{-1}$))]: 15.89 (1.84), 19.2 (2.1)^{sh}, 22.8 (2.8)^{sh}, 28.41 (3.87), 29.76 (3.88), 31.3 (4.0)^{sh}, 33.6 (4.2)^{sh}, 35.71 (4.49), 42.7 (4.6)^{sh}, 45.04 (4.72), 48.78 (4.69). CD spectrum in H_2O [ν_{max}, $10^3\,cm^{-1}$ ($\Delta\varepsilon$)]: 15.85 (+2.55), 19.42 (−10.13), 22.2 (+6.9)^{sh}, 25.4 (+16.2)^{sh}, 27.86 (+16.76), 31.5 (−35.8)^{sh}, 33.4 (−43.2)^{sh}, 35.84 (−89.21), 41.5 (−30.0)^{sh}, 44.05 (−48.44), 48.31 (−28.57). Diffuse reflectance spectrum [ν_{max}, $10^3\,cm^{-1}$]: 15.63, 19.1^{sh}, 22.4^{sh}, 28.09, 29.4^{sh}, 30.9^{sh}, 32.7^{sh}, 35.0^{sh}.

DphenPt · 2H$_2$O: yield = 0.30 g (70% based on Co). Anal. Calcd for $C_{22}H_{30}BN_4O_6F_4S_2CoPt$ (%): C, 31.03; H, 3.55; N, 6.58. Found (%): C, 31.03; H, 3.57; N, 6.51. ^{1}H-NMR (300 MHz, 1 : 1 mixed solvent of D_2O and CD_3CN), $\delta = 1.57$ (s, 6H, pen), 1.70 (s, 6H, pen), 3.89 (s, 2H, pen), 8.27 (t, 2H, phen), 8.29 (s, 2H, phen), 9.04 (d, 2H, phen), 9.39 (d, 2H, phen). UV-Vis spectrum in H_2O [ν_{max}, $10^3\,cm^{-1}$ ($\log\varepsilon$ ($mol^{-1}\,dm^3\,cm^{-1}$))]: 16.21 (2.02), 19.42 (2.09), 25.0 (3.2)^{sh}, 27.62 (3.76), 28.99 (3.80), 30.5 (3.9)^{sh}, 33.0 (4.2)^{sh}, 35.84 (4.52), 42.0 (4.4)^{sh}, 45.05 (4.64). CD spectrum in H_2O [ν_{max}, $10^3\,cm^{-1}$ ($\Delta\varepsilon$)]: 16.13 (−4.50), 19.42 (+7.42), 25.45 (−4.18), 27.4 (+6.4)^{sh}, 28.99 (+12.09), 29.94 (+12.06), 31.2 (+7.0)^{sh}, 35.71 (+44.72), 44.05 (+51.44). Diffuse reflectance spectrum [ν_{max}, $10^3\,cm^{-1}$]: 15.85, 19.16, 25.0^{sh}, 27.17, 28.3^{sh}, 30.0^{sh}, 32.4^{sh}, 34.8^{sh}.

LphenPt · 2H$_2$O: yield = 0.28 g (66% based on Co). Anal. Calcd for $C_{22}H_{30}BN_4O_6F_4S_2CoPt$ (%): C, 31.03; H, 3.55; N, 6.58. Found (%): C, 31.05; H, 3.55; N, 6.50. ^{1}H-NMR (300 MHz, 1 : 1 mixed solvent of D_2O and CD_3CN), $\delta = 1.58$ (s, 6H, pen), 1.70 (s, 6H, pen), 3.90 (s, 2H, pen), 8.27 (t, 2H, phen), 8.29 (s, 2H, phen), 9.04 (d, 2H, phen), 9.39 (d, 2H, phen). UV-Vis spectrum in H_2O [ν_{max}, $10^3\,cm^{-1}$ ($\log\varepsilon$ ($mol^{-1}\,dm^3\,cm^{-1}$))]: 16.18 (2.01), 19.38 (2.09), 25.0 (3.2)^{sh}, 27.62 (3.76), 28.99 (3.80), 30.5 (3.9)^{sh}, 33.0 (4.2)^{sh}, 35.84 (4.52), 42.0 (4.4)^{sh}, 45.05 (4.64). CD spectrum in H_2O [ν_{max}, $10^3\,cm^{-1}$ ($\Delta\varepsilon$)]: 16.10 (+4.43), 19.38 (−7.34), 25.45 (+4.16), 27.4 (−8.0)^{sh}, 28.99 (−12.79), 29.94 (−12.78), 31.1 $(-9.2)^{sh}$, 35.71 (−43.65), 44.25 (−51.49). Diffuse reflectance spectrum [ν_{max}, $10^3\,cm^{-1}$]: 15.87, 19.16, 25.0^{sh}, 27.17, 28.3^{sh}, 30.0^{sh}, 32.4^{sh}, 34.8^{sh}.

2.5. *Preparation of [M(phen){Co(D-pen)$_2$}]$_{0.5}$[M(phen){Co(L-pen)$_2$}]$_{0.5}$BF$_4$-A (DLphenM-A)*

The same synthetic procedure was employed as for the preparation of DLbpyM, except that an equimolar mixture of DphenM and LphenM was used instead of an equimolar mixture of DbpyM and LbpyM.

DLphenPd-A · 4H$_2$O: yield = 0.33 g (83% based on Co). Anal. Calcd for $C_{22}H_{34}BN_4O_8F_4S_2CoPd$ (%): C, 33.08; H, 4.29; N, 7.01. Found (%): C, 33.07; H, 4.31; N, 6.98. ^{1}H-NMR (300 MHz, 1:1 mixed solvent of D_2O and CD_3CN), $\delta = 1.59$ (s, 6H, pen), 1.83 (s, 6H, pen), 3.76 (s, 2H, pen), 8.21 (t, 2H, phen), 8.27 (s, 2H, phen), 8.96 (d, 2H, phen), 9.26 (d, 2H, phen). UV-Vis spectrum in H_2O [ν_{max}, $10^3\,cm^{-1}$ ($\log\varepsilon$ ($mol^{-1}\,dm^3\,cm^{-1}$))]: 15.80 (1.85), 19.2 $(2.1)^{sh}$, 22.8 $(2.8)^{sh}$, 28.41 (3.88), 29.76 (3.90), 31.3 $(4.0)^{sh}$, 33.6 $(4.3)^{sh}$, 35.71 (4.53), 42.7 $(4.6)^{sh}$, 45.46 (4.75), 48.78 (4.72). Diffuse reflectance spectrum [ν_{max}, $10^3\,cm^{-1}$]: 15.63, 21.6^{sh}, 27.96, 29.3^{sh}, 30.7^{sh}, 32.6^{sh}, 35.0^{sh}.

DLphenPt-A · 4H$_2$O: yield = 0.36 g (81% based on Co). Anal. Calcd for $C_{22}H_{34}BN_4O_8F_4S_2CoPt$ (%): C, 29.77; H, 3.86; N, 6.31. Found (%): C, 29.78; H, 3.85; N, 6.27. ^{1}H-NMR (300 MHz, 1 : 1 mixed solvent of D_2O and CD_3CN), $\delta = 1.57$ (s, 6H, pen), 1.69 (s, 6H, pen), 3.89 (s, 2H, pen), 8.26 (t, 2H, phen), 8.29 (s, 2H, phen), 9.03 (d, 2H, phen), 9.37 (d, 2H, phen). UV-Vis spectrum in H_2O [ν_{max}, $10^3\,cm^{-1}$ ($\log\varepsilon$ ($mol^{-1}\,dm^3\,cm^{-1}$))]: 16.10 (2.01), 19.31 (2.04), 25.0 $(3.2)^{sh}$, 27.62 (3.77), 28.99 (3.81), 30.5 $(3.9)^{sh}$, 33.0 $(4.2)^{sh}$, 35.84 (4.53), 42.0 $(4.4)^{sh}$, 45.04 (4.64). Diffuse reflectance spectrum [ν_{max}, $10^3\,cm^{-1}$]: 15.92, 19.34, 24.5^{sh}, 26.99, 28.4^{sh}, 29.9^{sh}, 32.1^{sh}, 34.0^{sh}.

2.6. *Preparation of [M(phen){Co(D-pen)$_2$}]$_{0.5}$[M(phen){Co(L-pen)$_2$}]$_{0.5}$BF$_4$-B (DLphenM-B)*

The same synthetic procedure was employed as for preparation of DLphenM-A, except that an equimolar mixture of DphenM and LphenM was dissolved in a minimum of a 1 : 1 mixed solvent of CH_3CN and H_2O, instead of H_2O.

DLphenPd-B · 4H$_2$O: yield = 0.30 g (75% based on Co). Anal. Calcd for $C_{22}H_{34}BN_4O_8F_4S_2CoPd$ (%): C, 33.08; H, 4.29; N, 7.01. Found (%): C, 33.09; H, 4.28; N, 6.96. ^{1}H-NMR (300 MHz, 1 : 1 mixed solvent of D_2O and CD_3CN), $\delta = 1.58$ (s, 6H, pen), 1.82 (s, 6H, pen), 3.75 (s, 2H, pen), 8.20 (t, 2H, phen), 8.26 (s, 2H, phen), 8.95 (d, 2H, phen), 9.25 (d, 2H, phen). UV-Vis spectrum in H_2O [ν_{max}, $10^3\,cm^{-1}$ ($\log\varepsilon$ ($mol^{-1}\,dm^3\,cm^{-1}$))]: 15.87 (1.76), 19.2 $(2.0)^{sh}$, 22.8 $(2.7)^{sh}$, 28.41 (3.78), 29.76 (3.80), 31.3 $(3.9)^{sh}$, 33.6 $(4.2)^{sh}$, 35.71 (4.44), 42.7 $(4.5)^{sh}$, 45.46 (4.66), 48.78 (4.62). Diffuse reflectance spectrum [ν_{max}, $10^3\,cm^{-1}$]: 15.63, 21.4^{sh}, 27.78, 29.2^{sh}, 30.6^{sh}, 32.5^{sh}, 35.0^{sh}.

DLphenPt-B · 4H$_2$O: yield = 0.34 g (77% based on Co). Anal. Calcd for $C_{22}H_{34}BN_4O_8F_4S_2CoPt$ (%): C, 29.77; H, 3.86; N, 6.31. Found (%): C, 29.77; H, 3.88; N, 6.25. ^{1}H-NMR (300 MHz, 1 : 1 mixed solvent of D_2O and CD_3CN), $\delta = 1.57$ (s, 6H, pen), 1.70 (s, 6H, pen), 3.90 (s, 2H, pen), 8.26 (t, 2H, phen), 8.29 (s, 2H, phen), 9.04 (d, 2H, phen), 9.39 (d, 2H, phen). UV-Vis spectrum in H_2O [ν_{max}, $10^3\,cm^{-1}$ ($\log\varepsilon$

(mol^{-1} dm^3 cm^{-1}))]: 16.16 (2.00), 19.42 (2.03), 25.0 (3.2)^{sh}, 27.62 (3.75), 28.99 (3.78), 30.5 (3.9)^{sh}, 33.0 (4.2)^{sh}, 35.84 (4.51), 42.0 (4.4)^{sh}, 45.04 (4.62). Diffuse reflectance spectrum [ν_{max}, 10^3 cm^{-1}]: 15.98, 19.38, 24.25^{sh}, 26.77, 28.3^{sh}, 29.7^{sh}, 32.0^{sh}, 34.2^{sh}.

2.7. *Measurements*

Electronic absorption spectra were recorded with a Perkin-Elmer Lambda 19 spectrophotometer and the CD spectra with a JASCO J-720 spectropolarimeter. These measurements were carried out in aqueous solutions at room temperature. Diffuse reflectance spectra were measured with a Perkin-Elmer Lambda 900 spectrophotometer equipped with an integrating sphere apparatus. ^{1}H-NMR spectra were recorded with a JEOL JNM-AL300 NMR spectrometer in a 1 : 1 mixed solvent of CD_3CN and D_2O using sodium 4,4-dimethyl-4-silapentane-1-sulfonate (DSS) as an internal reference. Elemental analyses (C, H, N) were performed with a Perkin-Elmer 2400 CHN Elemental Analyzer.

2.8. *X-ray structure determination*

Single crystals of DLbpyPd · $4H_2O$, DLbpyPt · $4H_2O$, DLphenPd-A · $4H_2O$, DLphenPd-B · $4H_2O$, DLphenPt-A · $4H_2O$, and DLphenPt-B · $4H_2O$ were used for data collection on a Rigaku AFC5S automated four-circle diffractometer with graphite-monochromated MoKα ($\lambda = 0.71069$ Å) radiation. Cell constants and an orientation matrix for data collection were obtained from least-squares refinement using the setting angles of 25 carefully centered reflections in the range $14° < \theta < 15°$ for DLbpyPd · $4H_2O$, DLbpyPt · $4H_2O$, DLphenPd-A · $4H_2O$, DLphenPd-B · $4H_2O$, DLphenPt-A · $4H_2O$, and DLphenPt-B · $4H_2O$. The data were collected at 296 ± 1 K using the ω-2θ scan technique to a maximum 2θ value of 55°. The weak reflections ($I < 10.0\,\sigma(I)$) were rescanned (maximum of three scans), and the counts were accumulated to ensure good counting statistics. Stationary background counts were recorded on each side of the reflection. The ratio of peak counting time to background counting time was 2 : 1. The intensities of three representative reflections were measured after every 150 reflections. Over the course of data collection, the standards decreased by <7.5%. Polynomial correction factors were applied to the data to account for this phenomenon. Empirical absorption corrections based on azimuthal scans of several reflections were applied. The data were corrected for Lorentz and polarization effects. The crystal data and experimental parameters are summarized in table 1. The structures were solved by direct methods for DLbpyPd · $4H_2O$, DLbpyPt · $4H_2O$, DLphenPd-A · $4H_2O$, DLphenPd-B · $4H_2O$, DLphenPt-A · $4H_2O$, and DLphenPt-B · $4H_2O$ and expanded using Fourier techniques [15, 16]. The non-hydrogen atoms were refined anisotropically. All hydrogens, except those of the water molecules which were not included in any of the structural models, were placed in calculated positions and refined with a riding model. The final cycle of full-matrix least-squares refinement on F^2 was based on observed reflections ($I > 2.00\sigma(I)$) and variable parameters, and converged with unweighted and weighted agreement factors of R and Rw. Neutral atom scattering factors were taken from Cromer and Waber [17]. Anomalous dispersion effects were included in Fc; the values for $\Delta f'$ and $\Delta f''$ were those of Creagh and McAuley [18–20]. All calculations were

Table 1. Crystallographic data for DLbpyPd · $4H_2O$, DLbpyPt · $4H_2O$, DLphenPd-A · $4H_2O$, DLphenPd-B · $4H_2O$, DLphenPt-A · $4H_2O$, and DLphenPt-B · $4H_2O$.

	DLbpyPd · $4H_2O$	DLbpyPt · $4H_2O$	DLphenPd-A · $4H_2O$	DLphenPd-B · $4H_2O$	DLphenPt-A · $4H_2O$	DLphenPt-B · $4H_2O$
Empirical formula	$C_{20}H_{34}BN_4O_8F_4S_2CoPd$	$C_{20}H_{34}BN_4O_8F_4S_2CoPt$	$C_{22}H_{34}BN_4O_8F_4S_2CoPd$	$C_{22}H_{34}BN_4O_8F_4S_2CoPd$	$C_{22}H_{34}BN_4O_8F_4S_2CoPt$	$C_{22}H_{34}BN_4O_8F_4S_2CoPt$
Formula weight	774.77	863.46	798.79	798.79	887.48	887.48
Crystal size (mm^3)	0.60 × 0.40 × 0.20	0.50 × 0.10 × 0.10	0.70 × 0.50× 0.50	0.75 × 0.40 × 0.30	0.80 × 0.80 × 0.70	0.50 × 0.50 × 0.50
Space group	$P\bar{1}$	$P\bar{1}$	$P2(1)/c$	$P2(1)/c$	$P2(1)/c$	$P2(1)/c$
Unit cell dimensions (Å,°)						
a	9.909(3)	9.912(2)	16.389(3)	10.910(5)	16.341(9)	10.857(7)
b	10.311(6)	10.305(2)	10.353(2)	34.514(8)	10.326(8)	34.286(8)
c	15.807(7)	15.786(2)	20.102(3)	8.401(4)	20.047(7)	8.342(8)
α	73.51(5)	73.44(1)	90	90	90	90
β	76.34(3)	75.96(2)	112.67(2)	97.57(4)	112.66(4)	97.00(6)
γ	72.94(4)	72.85(1)	90	90	90	90
Volume ($Å^3$), Z	1460(1), 2	1454.6(4), 2	3147.1(9), 4	3136(2), 4	3122(3), 4	3082(4), 4
Calculated density ($g\,cm^{-3}$)	1.763	1.971	1.686	1.692	1.888	1.912
Absorption coefficient (cm^{-1})	14.031	55.738	13.045	13.092	51.972	52.640
Transition factors	0.72–1.00	0.70–1.00	0.74–1.00	0.78–1.00	0.68–1.00	0.76–1.00
Total reflections	7087	7058	7490	7618	7425	7409
Reflection ($I > 2\sigma(I)$)	4758	5638	5844	5732	5732	5773
Number of variables	396	396	414	414	414	414
R (R_w)	0.0616 (0.1683)	0.0409 (0.0939)	0.0576 (0.1872)	0.0654 (0.2034)	0.0459 (0.1314)	0.0448 (0.1235)
Goodness-of-fit on F^2	1.002	1.008	1.004	1.002	1.012	1.011

performed using the Crystal Structure crystallographic software package of Molecular Structure Corporation [21, 22].

3. Results and discussion

3.1. *Crystal structures*

A mixture of equimolar amount of DbpyPt and LbpyPt in H_2O crystallizes as DLbpyPt · $4H_2O$ in the triclinic space group $P\bar{1}$ in marked contrast with the acentric space groups for crystals of optically active complexes, [Pt(bpy){Co(D-pen)$_2$}]X · nH_2O (X = Br^-, I^-, NO_3^-, or ClO_4^-) and [Pt(bpy){Co(L-pen)$_2$}]X · nH_2O, but essentially consistent with centric space groups for crystals of racemic complexes, [Pt(bpy){Co(D-pen)$_2$}]$_{0.5}$[Pt(bpy){Co(L-pen)$_2$}]$_{0.5}$X · nH_2O (table 1) [4, 6, 7]. Analogously, the remaining five racemic complexes, DLbpyPd · $4H_2O$, DLphenPd-A · $4H_2O$, DLphenPd-B · $4H_2O$, DLphenPt-A · $4H_2O$, and DLphenPt-B · $4H_2O$, crystallize in centric space groups from aqueous solutions containing D- and L-isomers in molar ratio of 1 : 1. Although the enantiomeric complex cations, D- and L-isomers, are included in the ratio of 1 : 1 in each crystal of DLbpyPd · $4H_2O$, DLbpyPt · $4H_2O$, DLphenPd-A · $4H_2O$, DLphenPd-B · $4H_2O$, DLphenPt-A · $4H_2O$, and DLphenPt-B · $4H_2O$, only one monovalent complex cation is a crystallographically independent component. Perspective drawings of L isomers of DLbpyPt · $4H_2O$ and DLphenPt-A · $4H_2O$ are shown in figure 1 as typical examples of the racemic DLLM (L = bpy or phen, M = Pd or Pt). Judging these two complex cations from outward appearance, there is no marked difference in structures except coordinated diimine ligands. In fact, as shown in table 2, there are no significant distinctions in the bond distances and angles around the Co(III) and Pt(II) atoms between DLbpyPt and DLphenPt-A. As compared with the previously reported optically active complexes, however, the Co(III) equatorial plane and PtS_2N_2 plane in DLbpyPt are somewhat bent (dihedral angle: 1.0°) and the PtS2N2 square-plane is rather distorted (dihedral angle between PtS_2 and PtN_2 planes: 3.6°). These facts suggest that some intermolecular interactions exist in the crystals of DLbpyPt · $4H_2O$. In DLbpyPt · $4H_2O$, a pair of enantiomeric complex cations, [Pt(bpy){Co(D-pen)$_2$}]$^+$ (*D*) and [Pt(bpy){Co(L-pen)$_2$}]$^+$ (*L*), forms a dimeric unit through π–π stacking of the bpy framework, with interplane distance between two π frameworks of 3.452 Å (figure 2a). Such a dimeric unit does not develop into a linear chain with further π–π stacking in contrast to racemic crystals with Cl^- and Br^- as counter anions, but in accord with those with I^-, NO_3^-, and ClO_4^- [4, 6, 7]. In DLbpyPt · $4H_2O$, the BF_4^- is located in the vicinity of one coordinated amino group of the octahedral Co(III) unit. As shown in figure 2a and table 3, for instance, N1 of the amino group is close to F1 of BF_4^-, accompanied by N1–H9 ··· F1 hydrogen bond formation. The hydrogen bonding amino group is opposite the π–π stacking phase. Additionally, the hydrogen bonding counter anion is overhung and extended to counteract further π–π stacking contacts with another bpy framework of the complex. The second hydrogen (H8) connected with N1 and H18 in another amino group form N1–H8 ··· O6 and N2–H18 ··· O5 hydrogen bonds, respectively. The remaining hydrogen, H17, is appropriated by a specific contact with the O1(a^1) atom of another adjacent enantiomeric complex cation, forming N2–H17 ··· O1(a^1) hydrogen bonds (figure 2b). These π–π stackings and hydrogen bonds between enantiomeric complex

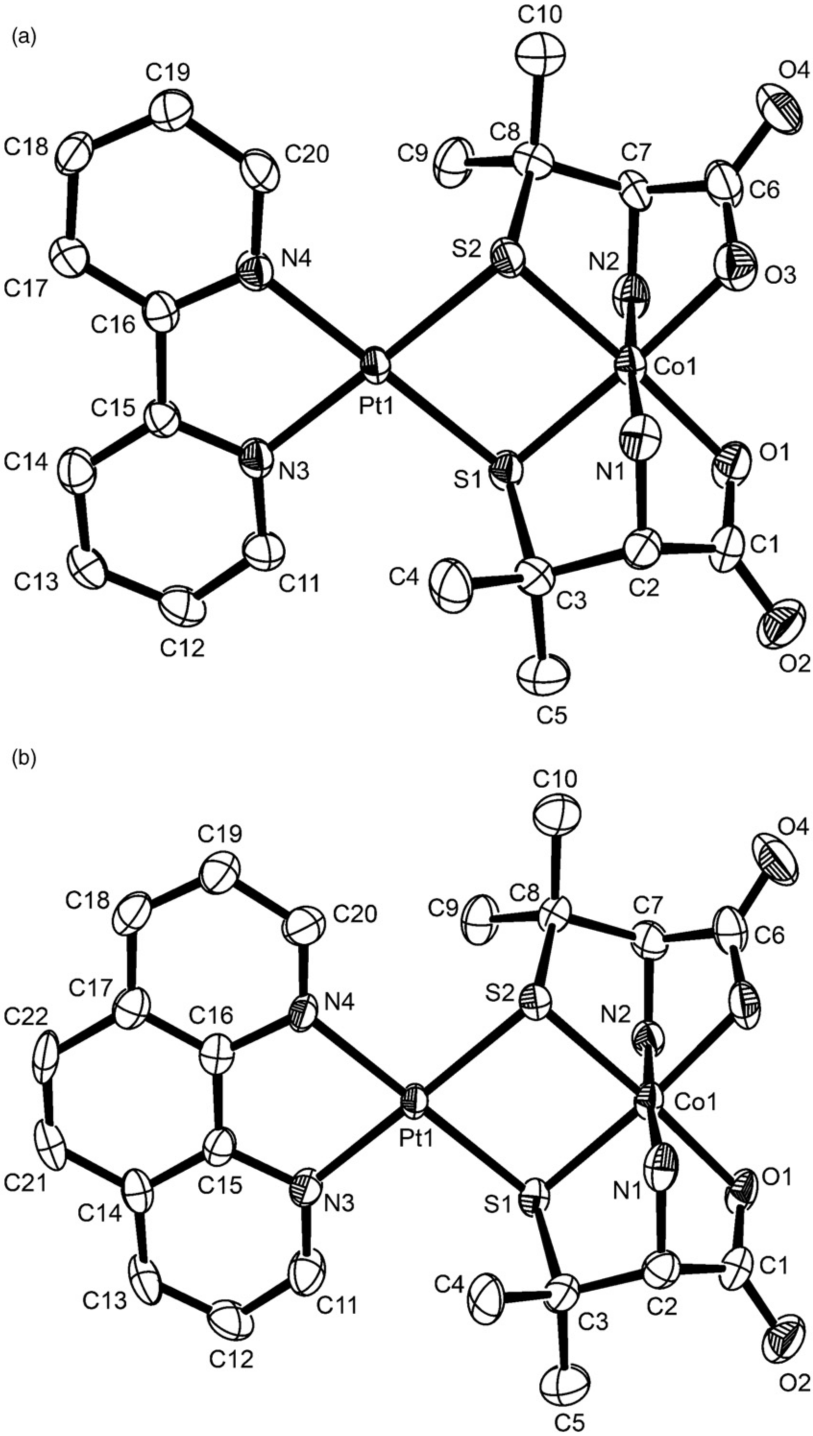

Figure 1. Perspective views of complex cations (L isomers) in (a) DLbpyPt · $4H_2O$ and (b) DLphenPt-A · $4H_2O$ with the atom labeling schemes (50% probability ellipsoids).

Table 2. Selected bond distances (Å) and angles (°) for DLbpyPd, DLbpyPt, DLphenPd-A, DLphenPd-B, DLphenPt-A, and DLphenPt-B.

	DLbpyPd	DLbpyPt	DLphenPd-A	DLphenPd-B	DLphenPt-A	DLphenPt-B
M1–S1	2.304(2)	2.302(2)	2.300(1)	2.299(2)	2.292(2)	2.290(2)
M1–S2	2.299(2)	2.299(2)	2.293(2)	2.295(2)	2.285(2)	2.292(2)
M1–N3	2.067(6)	2.058(5)	2.070(5)	2.086(6)	2.050(7)	2.060(6)
M1–M4	2.070(5)	2.043(5)	2.085(4)	2.085(5)	2.061(5)	2.053(6)
Co1–S1	2.226(2)	2.225(2)	2.228(2)	2.226(2)	2.223(2)	2.219(2)
Co1–S2	2.220(2)	2.222(2)	2.223(2)	2.220(2)	2.219(2)	2.220(2)
Co1–O1	1.946(4)	1.948(4)	1.944(3)	1.960(4)	1.940(5)	1.939(5)
Co1–O3	1.931(5)	1.925(5)	1.949(5)	1.948(5)	1.944(7)	1.957(6)
Co1–N1	1.939(6)	1.940(6)	1.959(4)	1.933(4)	1.949(6)	1.939(5)
Co1–N2	1.933(6)	1.928(6)	1.941(4)	1.941(5)	1.928(6)	1.941(6)
S1–M1–S2	83.10(6)	83.05(5)	82.99(5)	83.12(5)	83.03(7)	83.01(6)
S1–M1–N3	98.7(2)	99.0(1)	98.6(2)	98.1(2)	98.3(2)	98.2(2)
S1–M1–N4	178.5(2)	177.6(2)	178.7(1)	177.3(2)	178.6(2)	177.5(2)
S2–M1–N3	176.7(2)	176.7(2)	177.8(2)	177.4(2)	178.1(2)	177.0(2)
S2–M1–N4	97.9(2)	98.3(2)	97.6(2)	98.0(2)	97.6(2)	97.9(2)
N3–M1–N4	80.4(2)	79.7(2)	80.9(2)	80.9(2)	81.0(2)	81.0(2)
S1–Co1–S2	86.77(7)	86.60(6)	86.26(5)	86.54(6)	86.12(8)	86.33(7)
S1–Co1–O1	90.6(2)	91.1(2)	90.7(2)	90.7(2)	91.2(2)	90.8(2)
S1–Co1–O3	176.1(2)	176.6(2)	174.4(2)	175.5(1)	174.9(2)	175.6(2)
S1–Co1–N1	88.5(2)	88.0(2)	87.7(2)	87.8(2)	88.1(2)	87.3(2)
S1–Co1–N2	95.5(2)	95.6(2)	94.7(2)	96.7(2)	95.2(2)	96.4(2)
S2–Co1–O1	175.4(2)	175.8(2)	175.7(2)	176.3(1)	176.0(2)	176.3(2)
S2–Co1–O3	90.6 (2)	90.92	89.6(1)	89.2(2)	90.2(2)	89.3(2)
S2–Co1–N1	94.5(2)	94.0(2)	95.1(1)	94.8(2)	94.9(2)	94.7(2)
S2–Co1–N2	88.1(2)	88.2(2)	88.6(2)	88.8(2)	88.5(2)	89.1 (2)
O1–Co1–O3	92.2(2)	91.6(2)	93.6(2)	93.6(2)	92.7(2)	93.6(2)
O1–Co1–N1	81.6(2)	82.4(2)	81.7(2)	82.6(2)	82.1(2)	82.8(2)
O1–Co1–N2	96.0(2)	95.5(2)	94.8(2)	94.0(2)	94.7(2)	93.6(2)
O3–Co1–N1	94.6(2)	94.5(2)	96.4(2)	94.0(2)	95.6(2)	93.3(2)
O3–Co1–N2	81.4(2)	82.0(2)	81.4(2)	81.8(2)	81.2(2)	83.3(2)
N1–Co1–N2	175.3(2)	175.9(2)	175.8(2)	174.4(2)	175.4(3)	174.9(2)
M1–S1–Co1	94.91(6)	95.08(6)	95.20(5)	95.00(6)	95.27(7)	95.32(6)
M1–S2–Co1	95.21(7)	95.26(6)	95.54(5)	95.28(6)	95.58(8)	95.28(7)

cations result in a 1-D ladder-like network (figure 2c). The enantiomeric complex cations in DLbpyPd · $4H_2O$, DLphenPd-A · $4H_2O$, and DLphenPt-A · $4H_2O$, which crystallize from aqueous solution containing equimolar amounts of D- and L-isomers, also promote formations of the 1-D network through stereospecific dimeric π–π stacking between bpy or phen frameworks and hydrogen bonds between the octahedral Co(III) units (table 3).

Another type of racemic crystal, DLphenM-B · $4H_2O$, which has the same composition as the corresponding DLphenM-A · $4H_2O$ but exhibits a dissimilar lattice parameter, was obtained from aqueous acetonitrile solution containing D- and L-isomers in molar ratio of 1 : 1. Although the fundamental unit in DLphenPt-B · $4H_2O$ is a comparable π–π stacked dimer between D- and L-isomers, distributions of counter anions and/or water molecules of crystallizations around the coordinated amino groups are somewhat different from those in DLphenPt-A · $4H_2O$ (figure 3). Among four hydrogens (H8, H9, H17, H18) in two amino groups, H9 and H18 are accessible to O5 and O6 of water, respectively, forming N1–H9 ··· O5 and N2–H18 ··· O6 hydrogen bonds. While these two hydrogen bonds are located on sensitive sites to the π–π stacking, their expansions are much less than the hydrogen

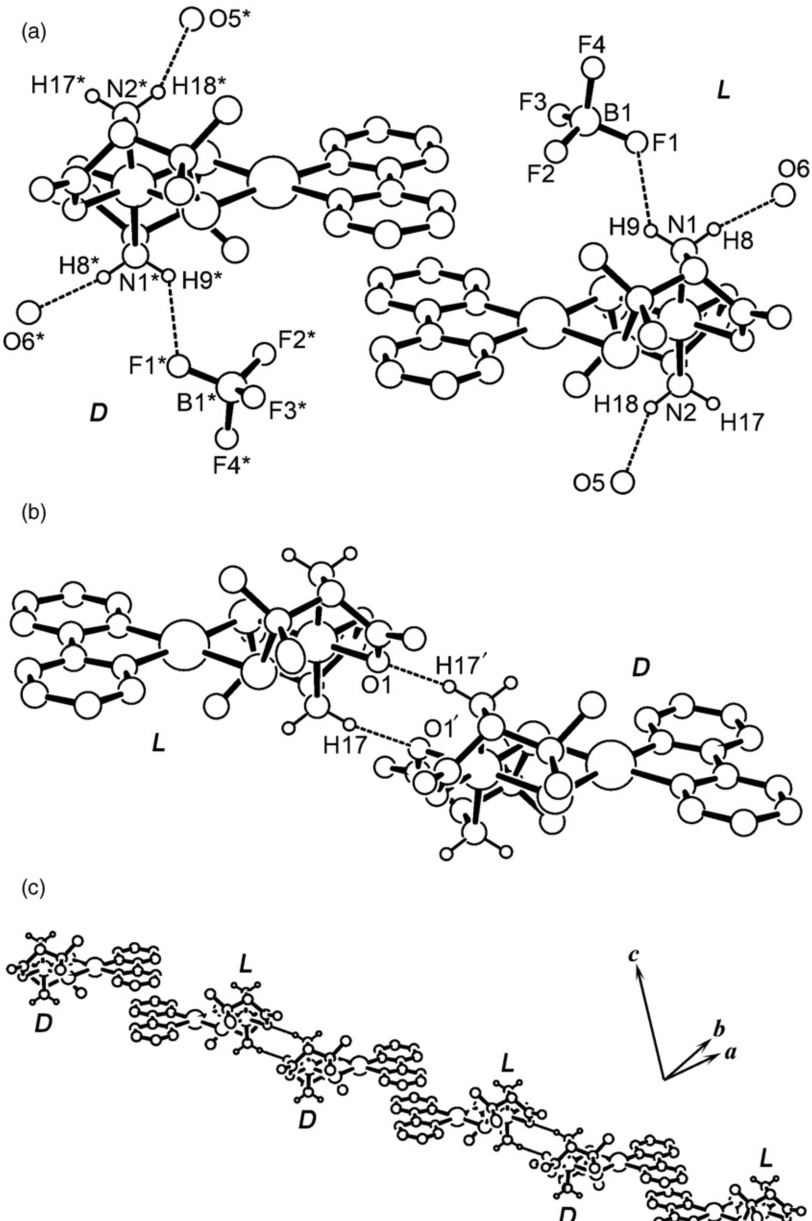

Figure 2. (a) Dimeric π–π stacking structure comprised of enantiomeric complex cations, D (D) and L (L) isomers, together with hydrogen bonding oxygens of water and contacting counter anions, in DLbpyPd $\cdot$ $4H_2O$. Symmetry code for asterisk: $x+1$, $y+1$, $z+1$. (b) Intermolecular hydrogen bonding structure of D (D) and L (L) isomers in DLbpyPd $\cdot$ $4H_2O$. Symmetry code for prime: $x+2$, $y+2$, z. (c) 1-D ladder-like network due to stereospecific π–π stackings and hydrogen bondings between enantiomeric complex cations in DLbpyPd $\cdot$ $4H_2O$.

Table 3. Hydrogen bonds of complex cations with counter anions, water molecules, or complex cations.

Complex	Interaction	$d(D\cdots A)$	$d(\tilde{D}H)$	$d(H\cdots A)$	$\angle$DHA
DLbpyPd	$N1-H8\cdots O6$	2.930	0.950	1.988	170.9
	$N1-H9\cdots F1$	3.029	0.950	2.300	133.0
	$N2-H17\cdots O1(a^1)$	2.916	0.950	2.044	151.9
	$N2-H18\cdots O5$	2.988	0.950	2.122	150.8
DLbpyPt	$N1-H8\cdots O6$	2.935	0.950	1.994	170.3
	$N1-H9\cdots F1$	3.020	0.950	2.323	129.7
	$N2-H17\cdots O1(b^1)$	2.901	0.950	2.036	150.6
	$N2-H18\cdots O5$	2.964	0.950	2.108	149.1
DLphenPd-A	$N1-H8\cdots O6$	2.940	0.950	2.015	163.8
	$N1-H9\cdots F1$	3.061	0.950	2.177	154.4
	$N2-H17\cdots O1(c^1)$	3.037	0.950	2.097	169.9
	$N2-H18\cdots O5$	2.882	0.950	1.998	154.0
DLphenPd-B	$N1-H8\cdots O1(d^1)$	3.034	0.950	2.096	169.0
	$N1-H9\cdots O5$	2.955	0.950	2.113	147.0
	$N2-H17\cdots O3(d^2)$	3.128	0.950	2.222	159.1
	$N2-H18\cdots O6$	2.969	0.950	2.115	148.7
	$O1\cdots H8(d^2)-N1(d^2)$	3.034	0.950	2.096	169.0
	$O3\cdots H17(d^1)-N2(d^1)$	3.128	0.950	2.222	159.1
DLphenPt-A	$N1-H8\cdots O6$	2.915	0.950	1.995	162.4
	$N1-H9\cdots F1$	3.039	0.950	2.167	152.1
	$N2-H17\cdots O1(e^1)$	3.036	0.950	2.098	168.9
	$N2-H18\cdots O5$	2.925	0.950	2.045	153.2
DLphenPt-B	$N1-H8\cdots O1(f^1)$	3.032(7)	0.950	2.094	169.3
	$N1-H9\cdots O5$	2.930(8)	0.950	2.107	144.2
	$N2-H17\cdots O3(f^2)$	3.080(8)	0.950	2.164	161.6
	$N2-H18\cdots O6$	2.962(13)	0.950	2.114	147.9
	$O1\cdots H8(f^2)-N1(f^2)$	3.032(7)	0.950	2.094	169.3
	$O3\cdots H17(f^1)-N2(f^1)$	3.080(8)	0.950	2.164	161.6

Symmetry codes: $a^1 = x+2, y+2, z$; $b^1 = x+1, y+3, z+1$; c^1: $-x+3, y+5/2, -z+7/2$; d^1: $x+1, y, z-1$; d^2: $x, y, z-1$; e^1: $x+1, y+2, z$; f^1: $x-1, y, z+1$; f^2: $x, y, z+1$.

bonded BF_4^- in DLphenPt-A $\cdot$ 4H_2O. This results in retention of sufficient space for further π–π stacking contacts to accord a linear chain structure for DLphenPt-B $\cdot$ 4H_2O. The remaining two hydrogens, H8 and H17, contribute to specific contacts with two different adjacent enantiomeric complex cations, forming $N1-H8\cdots O1(f^1)$ and $N2-H17\cdots O3(f^2)$ hydrogen bonds (figure 4a). As a result, a 2-D sheet-like network is built up with the π–π stackings and hydrogen bonds between the enantiomeric complex cations (figure 4b). A similar trend to DLphenPt-B $\cdot$ 4H_2O is also observed for the isostructural DLphenPd-B $\cdot$ 4H_2O. This is in contrast to DLbpyPd-A $\cdot$ 4H_2O or DLbpyPt-A $\cdot$ 4H_2O, for which only an identical complex crystallizes even from aqueous acetonitrile. It seems, therefore, that formations of 2-D sheet-like networks in DLphenPd-B $\cdot$ 4H_2O and DLphenPt-B $\cdot$ 4H_2O originate in the characteristic π electronic systems of the phen frameworks.

3.2. *Characterization*

In a 1 : 1 mixed solvent of CD_3CN and D_2O, DbpyPd exhibits ^{1}H-NMR signals at $\delta = 1.52$, 1.78, 3.69, 7.90, 8.37, 8.46, and 8.94. Among these signals, three at $\delta = 1.52$,

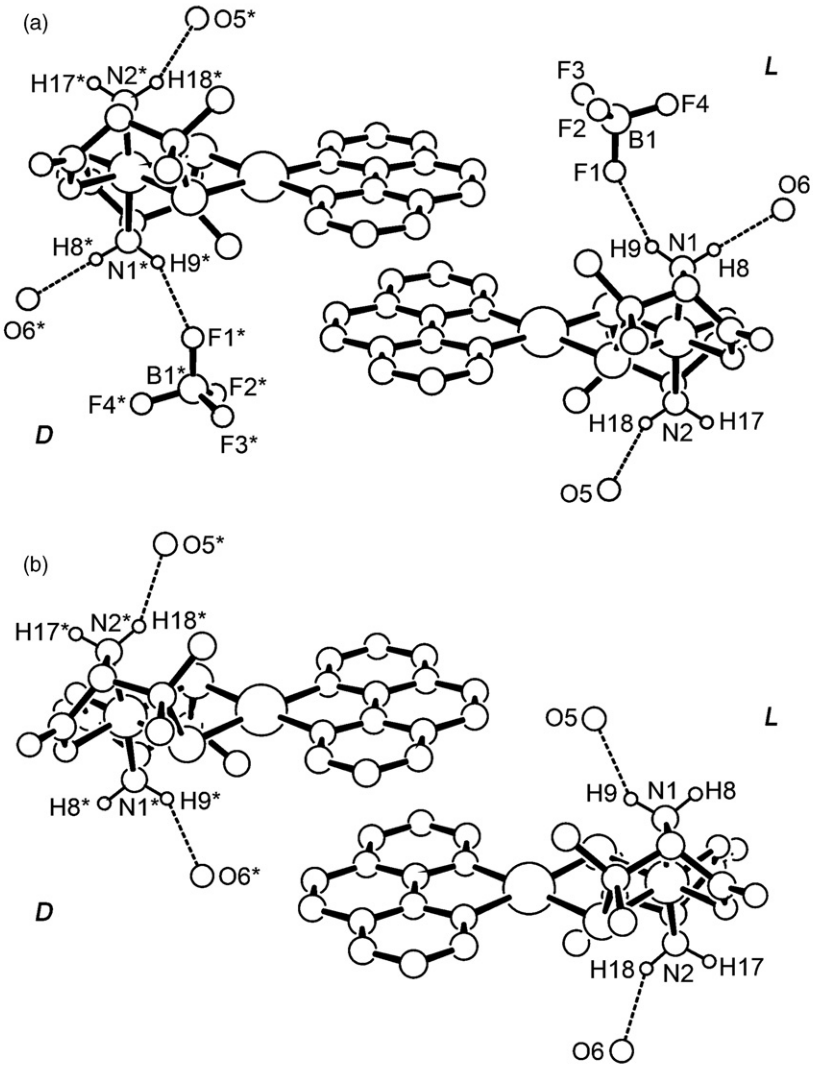

Figure 3. (a) Dimeric π–π stacking unit comprised of enantiomeric complex cations, D (*D*) and L (*L*) isomers, together with hydrogen bonding oxygen atoms of water molecules and contacting counter anions in DLphenPd-A $\cdot$ $4H_2O$. Symmetry code for asterisk: $-x+2$, $y+3/2$, $-z+7/2$. (b) The corresponding unit in DLphenPd-B $\cdot$ $4H_2O$. Symmetry code for asterisk: $-x+3$, $-y+2$, $-z+1$.

1.78, and 3.69 are attributable to the D-pen ligands [1, 3, 4, 6, 7, 23, 24]. The remaining four signals at $\delta = 7.90$, 8.37, 8.46, and 8.94 are ascribed as the bpy ligand [1–7, 9]. Similarly, ^{1}H-NMR spectrum of DbpyPt is comprised of three signals at $\delta = 1.50$, 1.66, and 3.83 due to D-pen ligands, and five signals at $\delta = 7.95$, 8.45, 8.50, and 9.08 due to bpy. Differences in chemical shifts between DbpyPd and DbpyPt reflect the incorporated square-planar d^8 metals into the S-bridged dinuclear structures. The ^{1}H-NMR spectrum of DphenPd also exhibits characteristic signals for D-pen ligands of the Co(III) unit bridging Pd(II) [2, 3, 7]. Additional signals due to the coordinated phen ligand to Pd(II)

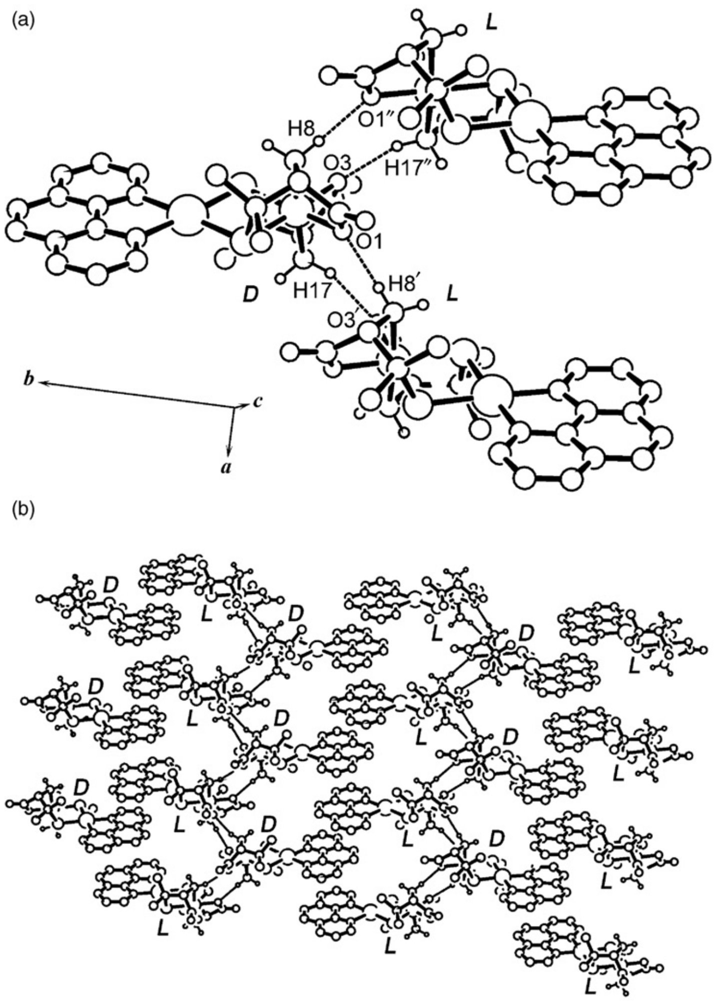

Figure 4. (a) Intermolecular hydrogen bonding structure of D (*D*) and L (*L*) isomers in DLphenPd-B $\cdot$ $4H_2O$. Symmetry codes for prime: x, y, $z-1$; double prime: $x+1$, y, $z-1$. (b) 2-D sheet-like networks due to stereospecific π–π stackings and hydrogen bondings between enantiomeric complex cations in DLphenPd-B $\cdot$ $4H_2O$.

were observed for DphenPd [9]. Similar to DphenPd, DphenPt shows the corresponding ^{1}H-NMR signals to the D-pen ligands of Co(III) unit bridging Pt(II) and the coordinated phen to Pt(II). It can be regarded, therefore, that DphenPd and DphenPt retain similar sulfur-bridged dinuclear structures to those in crystalline states. Optically active complexes with L-pen ligands, LbpyPd, LbpyPt, LphenPd, and LphenPt, exhibit almost identical spectral behavior with the corresponding D isomers, DbpyPd, DbpyPt, DphenPd, and DphenPt. Although two kinds of complex cations, [Pd(bpy){Co(D-pen)$_2$}]$^+$ and [Pd(bpy){Co(L-pen)$_2$}]$^+$, exist in DLbpyPd, on the other hand, the ^{1}H-NMR spectrum exhibits three signals due to the pen ligands and four signals characteristic for bpy. Furthermore, the spectral pattern of DLbpyPd is quite similar to those of DbpyPd and LbpyPd. Similarly, the NMR spectral behavior of DLbpyPt is

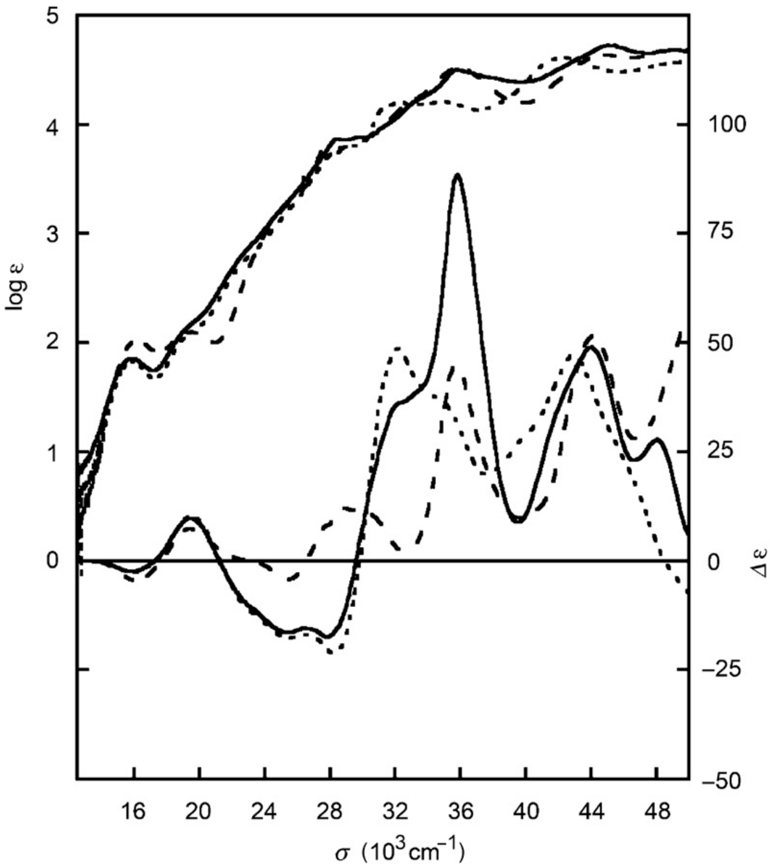

Figure 5. Electronic absorption and CD spectra of DbpyPd (dotted line), DphenPd (solid line), and DphenPt (broken line) in H_2O.

almost identical with that of DbpyPt or LbpyPt. These facts indicate no intermolecular interactions in these conditions, namely, concentrations of $10^{-2}\,\mathrm{mol\,dm^{-3}}$. It seems, therefore, that each enantiomeric complex cation in DLbpyPd or DLbpyPt exists as a monomer in solution as well as DbpyPd, LbpyPd, DbpyPt, or LbpyPt. The ^{1}H-NMR spectrum of DLphenM-A (M = Pd or Pt) can be equated with that of DLphenM-B (M = Pd or Pt), while DLphenM-A and DLphenM-B provide distinguishable π–π stacking interactions in the crystalline state. In addition, the spectral behaviors of DLphenM-A and DLphenM-B are rather analogous with those of DphenM and LphenM. Therefore, each enantiomeric complex cation in DLphenM-A and DLphenM-B exists as a monomer in solution as well as DLbpyPd and DLbpyPt.

Electronic absorption and CD spectra of DbpyM, LbpyM, and DLbpyM (M = Pd, Pt) in H_2O correspond to those of the previously reported [M(bpy){Co(D-pen)$_2$}]X $\cdot$ nH$_2$O ($X = Cl^-, Br^-, I^-, NO_3^-, ClO_4^-$), [M(bpy){Co(L-pen)$_2$}]X $\cdot$ nH$_2$O, and [M(bpy){Co(D-pen)$_2$}]$_{0.5}$[M(bpy){Co(L-pen)$_2$}]$_{0.5}$X $\cdot$ nH$_2$O, respectively [1, 3, 4, 6, 7]. In addition, the absorption spectrum of DLbpyM is well accorded with that of DbpyM or LbpyM, implying that all complexes behave as monomeric dinuclear complexes in H_2O.

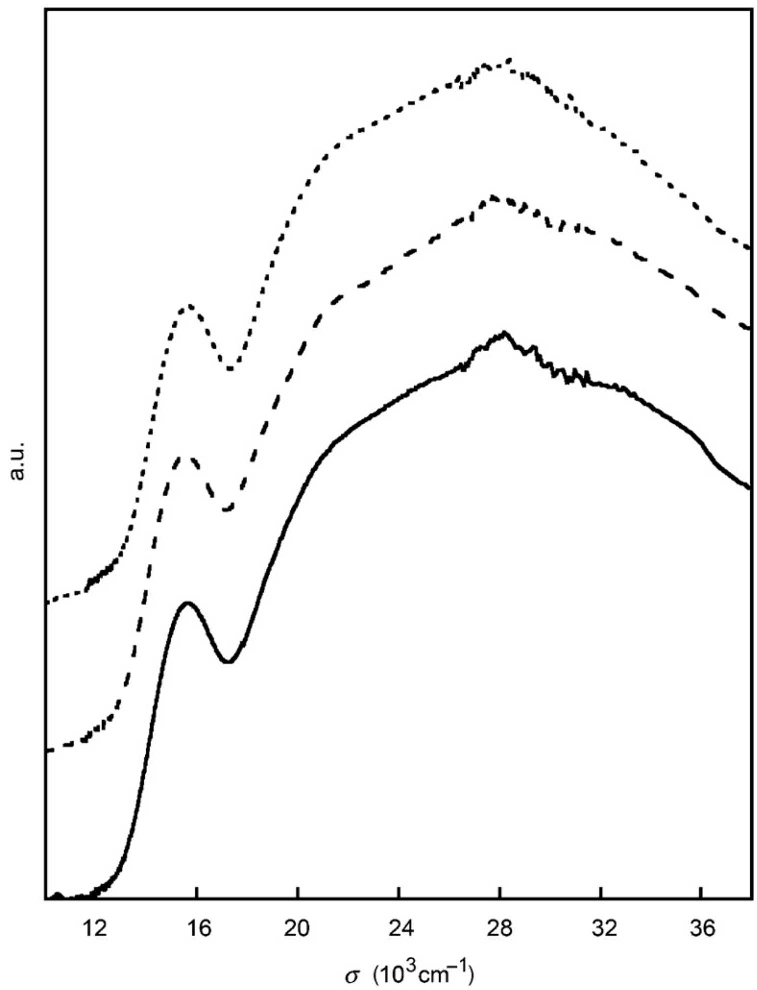

Figure 6. Diffuse reflectance spectra of DphenPd (solid line), DLphenPd-A (broken line), and DLphenPd-B (dotted line).

As shown in figure 5, the absorption spectrum of DphenPd is comprised of three components at 15.85, 19.2, and $22.8 \times 10^3\,cm^{-1}$. Additional bands due to the second d–d and sulfur-to-metal charge-transfer transitions are observed at 28.41 and $35.59 \times 10^3\,cm^{-1}$. These features are common to DbpyPd, while the spectra are different from each other in the region $29-34 \times 10^3\,cm^{-1}$. In this region, DphenPd shows three bands at 29.76, 31.3, and $33.6 \times 10^3\,cm^{-1}$. The corresponding absorption bands also appear in the spectra of the other sulfur-bridged polynuclear Pd complexes with coordinated phen ligands [9]. This implies that the bands at 29.76, 31.3, and $33.6 \times 10^3\,cm^{-1}$ are ascribed as intraligand π–π* transitions in the phen framework of DbpyPd. The corresponding three π–π* bands in DphenPt are slightly shifted toward the lower energy side and observed at 28.99, 30.5, and $33.0 \times 10^3\,cm^{-1}$, reflecting the incorporated square-planar d^8 metals into the S-bridged dinuclear structures.

The absorption spectral profiles of LphenPd and LphenPt are essentially consistent with those of DphenPd and DphenPt, respectively, reflecting the enantiomeric relationships between the complexes. Although DLphenM-A and DLphenM-B involve two enantiomeric components and have dimeric or linear-chain π–π stacking structures in the crystalline state, the spectra are hardly distinguishable from each other. Furthermore, their spectral patterns are quite similar to the corresponding DphenM and LphenM. These results also do not support significant interaction between DLphenM-A and DLphenM-B in H_2O. The CD spectrum of DphenPd is comprised of seven positive bands at 19.42, 31.9, 33.1, 35.84, 41.8, 44.05, and $48.08 \times 10^3\,cm^{-1}$, and five negative bands at 15.80, 22.3, 25.5, 27.86, and $31.9 \times 10^3\,cm^{-1}$. While the positions and absolute values of strengths of these CD bands for LphenPd correspond well with those for DphenPd, each sign is opposite to the corresponding signs of LphenPd on the basis of the enantiomeric relationship. A similar spectral relationship is also observed between DphenPt and LphenPt. In contrast to the optically active DphenM and LphenM, DLphenM-A, and DLphenM-B in H_2O show no CD signals over the whole region. It can be concluded, therefore, that crystals of DLphenM-A and DLphenM-B involve accurately equimolecular amounts of DphenM and LphenM.

Diffuse reflectance spectra of the optically active DbpyM and LbpyM correspond well with the absorption spectra in H_2O. Such spectral behaviors are commonly observed features for $[M(bpy)\{Co(\text{D-pen})_2\}]X \cdot nH_2O$ ($X = Cl^-, Br^-, I^-, NO_3^-, ClO_4^-$) and $[M(bpy)\{Co(\text{L-pen})_2\}]X \cdot nH_2O$ without π–π stacking even in the crystalline states [1, 3, 4, 6, 7]. In the same way, the reflectance spectra of the optically active DphenM and LphenM are coincident with their solution absorption spectra. In DphenPd, for instance, the 15.63, 19.1, 22.4, 28.09, 29.4, 30.9, 32.7, and $35.0 \times 10^3\,cm^{-1}$ reflectance bands are compatible with the 15.85, 19.2, 22.8, 28.41, 29.76, 31.3, 33.6, and $35.59 \times 10^3\,cm^{-1}$ absorption bands (figure 6). Therefore, each complex cation in DphenM (LphenM) as well as DbpyM (LbpyM) is relieved of π–π stacking interaction. In the racemic DLbpyM, on the other hand, the reflectance spectral profiles are slightly different from the absorption ones. Furthermore, the reflectance spectra of DLbpyM are distinguishable from those of DbpyM and LbpyM. The exact same trends are recognized for $[M(bpy)\{Co(\text{D-pen})_2\}]_{0.5}[M(bpy)\{Co(\text{D-pen})_2\}]_{0.5}X \cdot nH_2O$ ($X = I^-, NO_3^-, ClO_4^-$) and originated from dimeric π–π stacking interactions between enantiomeric complex cations [6]. Similar spectral deviations to DLbpyM are observed for the racemic DLphenM-A with dimeric π–π stacking arrangements in the crystalline state. This is illustrated by an example of DLphenPd-A, in which localized electronic bands on phen frameworks appear at 29.3, 30.7, and $32.6 \times 10^3\,cm^{-1}$ (figure 6). These three reflectance bands of DLphenPd-A are at lower energy than the corresponding bands of DphenPd or LphenPd. Furthermore, DLphenPd-A shows only one shoulder ($21.6 \times 10^3\,cm^{-1}$) in the region of $19–24 \times 10^3\,cm^{-1}$, while DphenPd or LphenPd possesses two distinct reflectance bands in this region. Such characteristic behavior for the racemic crystals emerges emphatically in DLphenM-B with linear-chained π–π stacking structures in the crystalline states. In DLphenPd-B, more specifically, the corresponding reflectance bands to localized electronic transitions on phen frameworks shift further to lower energy at 29.2, 30.6, and $32.6 \times 10^3\,cm^{-1}$. It can be concluded, therefore, that electronic natures of π frameworks in phen complexes change with configurations of π–π stackings, i.e., monomer, dimer, or linear chain.

4. Conclusions

The optically active Co(III) complexes, *trans*(N)-[Co(D-pen)$_2$]$^-$ (pen = penicillaminate) or *trans*(N)-[Co(L-pen)$_2$]$^-$, are sulfur-donating bidentate metalloligands, and hence react with [MCl$_2$(L)] {M = Pd or Pt, L = 2,2′-bipyridine (bpy) or 1,10-phenanthroline (phen)} in the presence of tetrafluoroborate to form a chiral sulfur-bridged dinuclear complex, [M(L){Co(D-pen)$_2$}]BF$_4 \cdot$ 2H$_2$O or [M(L){Co(L-pen)$_2$}]BF$_4 \cdot$ 2H$_2$O. Mixing these enantiomers in molar ratio 1 : 1 in aqueous media leads to formation of racemic crystals, [M(L){Co(D-pen)$_2$}]$_{0.5}$[M(L){Co(L-pen)$_2$}]$_{0.5}$BF$_4 \cdot$ 4H$_2$O. For racemic crystals with L = phen, two different polymorphs can be obtained depending on solvent (water with or without acetonitrile) used for crystallization. In the racemic crystals grown from water, [M(phen){Co(D-pen)$_2$}]$^+$ and [M(phen){Co(L-pen)$_2$}]$^+$ interact stereospecifically with each other through π-conjugated systems to form dimeric structures. [M(phen){Co(D-pen)$_2$}]$^+$ and [M(phen){Co(L-pen)$_2$}]$^+$ are arranged alternately while overlapping the phen planes form linear-chained π–π stacking structures in the racemic crystals grown from aqueous acetonitrile. Stereospecific hydrogen bonds between coordinated $-$NH$_2$ and $-$COO$^-$ groups are also formed in these two different polymorphs, while their bonding modes differ noticeably from each other. As a result, 1-D ladder-like networks are built up due to stereospecific π–π stackings and hydrogen bondings between enantiomers in the racemic crystals grown from water. In contrast, 2-D sheet-like networks are established for the racemic crystals grown from aqueous acetonitrile. These structural differences reflect their diffuse reflectance spectral behaviors.

Supplementary material

CCDC-744667 for DLbpyPd $\cdot$ 4H$_2$O, -744668 for DLbpyPt $\cdot$ 4H$_2$O, -744669 for DLphenPd-A $\cdot$ 4H$_2$O, -744670 for DLphenPt-A $\cdot$ 4H$_2$O, -744671 for DLphenPd-B $\cdot$ 4H$_2$O, and -744672 for DLphenPt-B $\cdot$ 4H$_2$O contain the supplementary crystallographic data for this article. These data can be obtained free of charge at www.ccdc.cam.ac.uk/conts/retrieving.html [or from the Cambridge Crystallographic Data Centre, 12, Union Road, Cambridge CB2 1EZ, UK; Fax: +44 1223 336 033; Email: deposit@ccdc.cam.ac.jk].

References

[1] Y. Yamada, M. Uchida, Y. Miyashita, K. Fujisawa, T. Konno, K. Okamoto. *Bull. Chem. Soc. Jpn.*, **73**, 913 (2000).
[2] Y. Yamada, Y. Maeda, T. Konno, K. Fujisawa, K. Okamoto. *Bull. Chem. Soc. Jpn.*, **73**, 1831 (2000).
[3] Y. Yamada, M. Uchida, M. Fujita, Y. Miyashita, K. Okamoto. *Polyhedron*, **22**, 1507 (2003).
[4] Y. Yamada, K. Okamoto. *Inorg. Chim. Acta*, **359**, 3963 (2006).
[5] Y. Yamada, M. Noda, M. Inoue, Y. Miyashita, K. Okamoto, M. Koikawa, T. Tokii. *J. Coord. Chem.*, **60**, 607 (2007).
[6] Y. Yamada, M. Inoue, Y. Miyashita, K. Okamoto, M. Koikawa, T. Tokii. *Polyhedron*, **26**, 2749 (2007).
[7] Y. Yamada, M. Inoue, K. Okamoto. *J. Coord. Chem.*, **61**, 1385 (2008).
[8] Y. Yamada, K. Okamoto. *Chem. Lett.*, **28**, 315 (1999).
[9] Y. Yamada, K. Fujisawa, K. Okamoto. *Bull. Chem. Soc. Jpn.*, **73**, 2067 (2000).
[10] Y. Yamada, K. Fujisawa, K. Okamoto. *Bull. Chem. Soc. Jpn.*, **73**, 2297 (2000).

[11] K. Okamoto, K. Wakayama, H. Einaga, S. Yamada, J. Hidaka. *Bull. Chem. Soc. Jpn.*, **56**, 165 (1983).
[12] N. Baidya, D. Ndreu, M. Olmstead, K. Mascharak. *Inorg. Chem.*, **30**, 2448 (1991).
[13] R.H. Herber, M. Croft, M.J. Coyer, B. Bilash, A. Sahiner. *Inorg. Chem.*, **33**, 2422 (1994).
[14] K. Okamoto, Y. Yoshinari, Y. Yamada, N. Sakagami, T. Konno. *Bull. Chem. Soc. Jpn.*, **71**, 1363 (1998).
[15] *SIR92*: A. Altomare, G. Cascarano, C. Giacovazzo, A. Guagliardi, M. Burla, G. Polidori, M. Camalli. *J. Appl. Cryst.*, **27**, 435 (1994).
[16] P.T. Beurskens, G. Admiraal, G. Beurskens, W.P. Bosman, R. de Gelder, R. Israel, J.M.M. Smits. *DIRDIF99. The DIRDIF 99 program system*, Technical Report of the Crystallography Laboratory, University of Nijmegen, The Netherlands (1999).
[17] D.T. Cromer, J.T. Waber (Eds.). *International Tables for X-ray Crystallography*, Vol. IV, Table 2.2 A, The Kynoch Press, Birmingham, England (1974).
[18] J.A. Ibers, W.C. Hamilton. *Acta Cryst.*, **17**, 781 (1964).
[19] D.C. Creagh, W.J. McAuley. In *International Tables for Crystallography*, A.J.C. Wilson (Ed.), Vol. C, pp. 219–222, Kluwer Academic Publishers, Boston (1992).
[20] D.C. Creagh, J.H. Hubbell. In *International Tables for Crystallography*, A.J.C. Wilson (Ed.), Vol. C, pp. 200–206, Kluwer Academic Publishers, Boston (1992).
[21] *CrystalStructure 3.8: Crystal Structure Analysis Package*, Rigaku and Rigaku Americas, 9009 New Trails Dr., The Woodlands, TX 77381, USA (2000–2007).
[22] J.R. Carruthers, J.S. Rollett, P.W. Betteridge, D. Kinna, L. Pearce, A. Larsen, E. Gabe. *CRYSTALS Issue 11*, Chemical Crystallography Laboratory, Oxford, UK (1999).
[23] Y. Yamada, M. Tsumita, A. Hirano, Y. Miyashita, K. Fujisawa, K. Okamoto. *Inorg. Chim. Acta*, **332**, 108 (2002).
[24] Y. Yamada, A. Hirano, M. Fujita, N. Amir, Y. Miyashita, K. Okamoto. *Inorg. Chim. Acta*, **358**, 667 (2005).